EQUILIBRIUM CONTROL VECTORS SUBSERVING RAPID GOAL-DIRECTED ARM MOVEMENTS

J.R. FLANAGAN[1], A.G. FELDMAN[2], and D.J. OSTRY[1]
[1]*McGill University, Montreal, Canada*
[2]*Institute for Information Transmission Problems, Moscow, U.S.S.R.*

ABSTRACT. The composition of central commands underlying rapid goal-directed arm movements to visual targets was explored within the framework of the equilibrium point hypothesis. This hypothesis suggests that movements arise from shifts in equilibrium associated with the dynamic interaction of central commands, reflex mechanisms, muscle properties, and loads. Central commands control this process by regulating muscle threshold lengths (λs) for motoneuron recruitment. Subjects performed rapid arm movements to fixed and displaced targets (LEDs) located in a horizontal plane. The position of the first target and the onset and the position of the second target were varied. Experimental trajectories of the movement endpoint (e.g., the hand or wrist) were compared with simulated trajectories, based on the λ model, generated with theoretical central commands. The findings support the hypothesis that multi-joint arm motions are planned in equilibrium coordinates corresponding to the position of the endpoint. Moreover, the results suggest that, in the absence of overriding constraints, the equilibrium position of the hand is shifted at a constant velocity towards the target. Finally, for rapid movements the rate of shift appears to be the same for movements of different amplitude.

1. Introduction

In this paper we describe experiments in which subjects made goal-directed arm movements to both single-step and double-step targets (LEDS) located in a horizontal plane. Subjects were asked to move rapidly to the presently illuminated target. For the double-step targets different inter-stimulus intervals (ISIs) were used ranging from 50 ms to 700 ms. Thus in some cases the target was shifted prior to the onset of movement whereas in other cases the second target was presented after the movement to the initial target was completed. We also present simulation data generated from a model of two-joint planar arm motion which is based on the equilibrium point (EP) hypothesis. A summary review of the EP hypothesis (λ model) - at the level of a single muscle and at the level of a single joint - is provided.

Figure 1 illustrates several aspects of the λ model at the level of a single muscle acting against a load. Five limb configurations are depicted in Figure 1a. The corresponding levels of depolarization of the motoneurons (MNs) innervating the muscle are shown in Figure 1b. The dashed horizontal line is the depolarization threshold (T_1) at which the first MN is recruited. As the level of depolarization increases beyond this threshold, the number of recruited MNs as well as their firing rates also increase. The level of depolarization of MNs is assumed to depend on the summation of central facilitation (open box) and afferent facilitation (filled box).

In A the system is in equilibrium with muscle length x_a. The level of MN depolarization (T_{L1}) exceeds threshold - with some specific combination of central and afferent facilitation - such that

J. Requin and G. E. Stelmach (eds.), Tutorials in Motor Neuroscience, 357–367.

Figure 1a

Figure 1: Single Muscle & Load

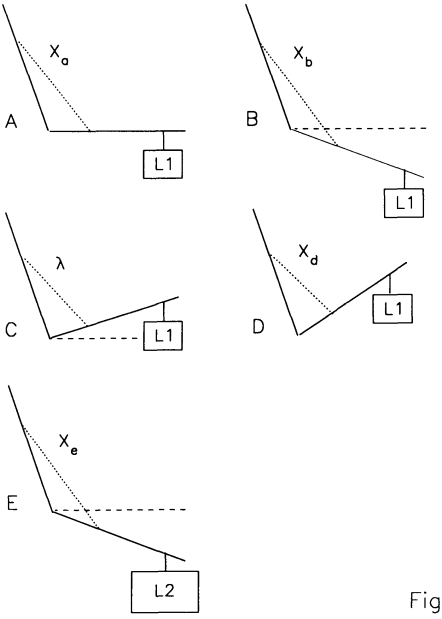

Figure 1b

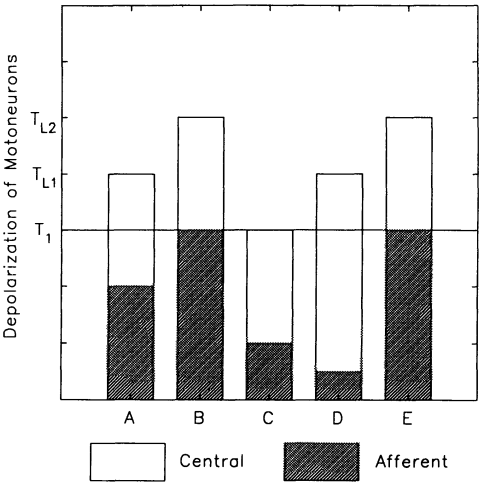

Figure 1

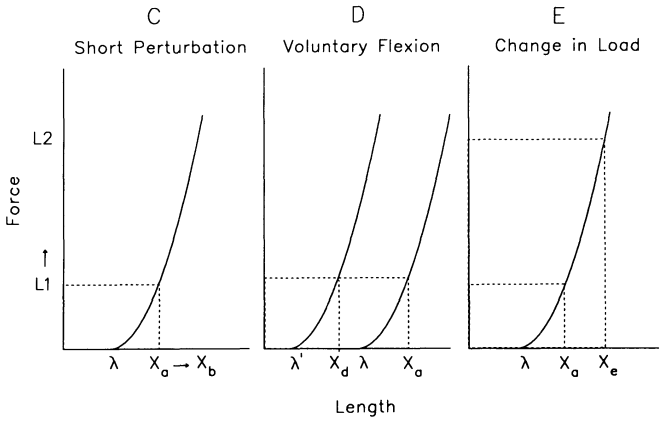

MNs are recruited and muscle force balances the load L1. Consider, in B, the response of the system to a short perturbation which stretches the muscle to length x_b. Due to muscle stretch the level of length dependent afferent facilitation increases, more MNs are recruited, and a flexion torque results which restores the system's equilibrium position to A. Now consider, in C, the response of the system to a brief perturbation which shortens the muscle. Afferent facilitation decreases, the level of depolarization is reduced, MNs are de-recruited, and the load acts to restore the system's equilibrium position. In this particular example, the muscle is shortened to the *recruitment threshold length* - denoted λ - at which all MNs are de-recruited. A biomechanical account of A-C is presented in Figure 1c which shows the muscle force-length curve. Initially the muscle is at length x_a corresponding to force L1. The muscle is then stretched to length x_b and the resulting force exceeds the load. Finally, in C, the muscle is shortened to the threshold length λ and zero force is produced. Figure 1c shows that all possible equilibrium states of the system associated with a constant level of central facilitation can be characterized by an invariant force-length curve which is defined by λ. Thus, the λ parameter is a position or load independent measure of the level of central facilitation.

Now consider, in D, how the nervous system produces a voluntary flexion motion (from A to D). The level of central facilitation is increased so that depolarization increases and more MNs are recruited. The muscle actively shortens to length x_d and length dependent afferent facilitation diminishes. For simplicity, we assume that the load is independent of limb position and that the same level of muscle activation is required to balance the load regardless of muscle length. Thus, when the sum of central and afferent facilitation is restored to the same level as in A, a new equilibrium position is established in which the load is once again balanced. The force-length curves corresponding to A and D are shown in Figure 1d. The effect of increasing central facilitation is to shorten the recruitment threshold length of the muscle from λ to λ'.

In A and D the same load is supported in two different positions with equivalent levels of MN activity. The sole difference between A and D is the relative amounts of central and afferent facilitation. Clearly, models which suggest that MN recruitment (i.e., muscle activity) is directly controlled by the nervous system fail to explain how the system differentiates between postures A to D.

Finally, in E, we may consider how the system in A reacts to a larger load L2. The muscle is stretched to length x_e, the level of afferent facilitation increases, and more MNs are recruited. This effect is illustrated in Figure 1e. Note that the load is balanced without changing the level of central facilitation (i.e., λ). Figure 1E illustrates how, for a given level of central facilitation, afferent feedback establishes a specific mapping between external space (i.e., muscle length) and MN activation. In the deafferented system, this elegant correspondence is lost. In this case, MN activity must be directly (centrally) controlled in order to generate movement. For example, in E, the level of central facilitation would be higher than in A in the deafferented system unlike the normal system. Under normal conditions, however, the model attributes an essential role to afferent regulation of MN activity in the control of posture and movement.

A simple single-joint system with a flexor and an extensor muscle is shown in Figure 2a. The joint angle Θ is defined such that it increases with joint extension. The corresponding torque-angle relationships for both the flexor and extensor muscles are presented in Figure 2b. The system is in static equilibrium; the torque produced by the flexor is equal and opposite to the torque produced by the extensor. Thus, the equilibrium joint angle (R) is specified by the combined actions of both muscles and corresponds to the angle at which the net joint torque is zero. The location of the flexor and extensor torque-angle curves is determined by the threshold lengths for the flexor (λ_f) and extensor (λ_e). Consider now the effects of briefly perturbing the

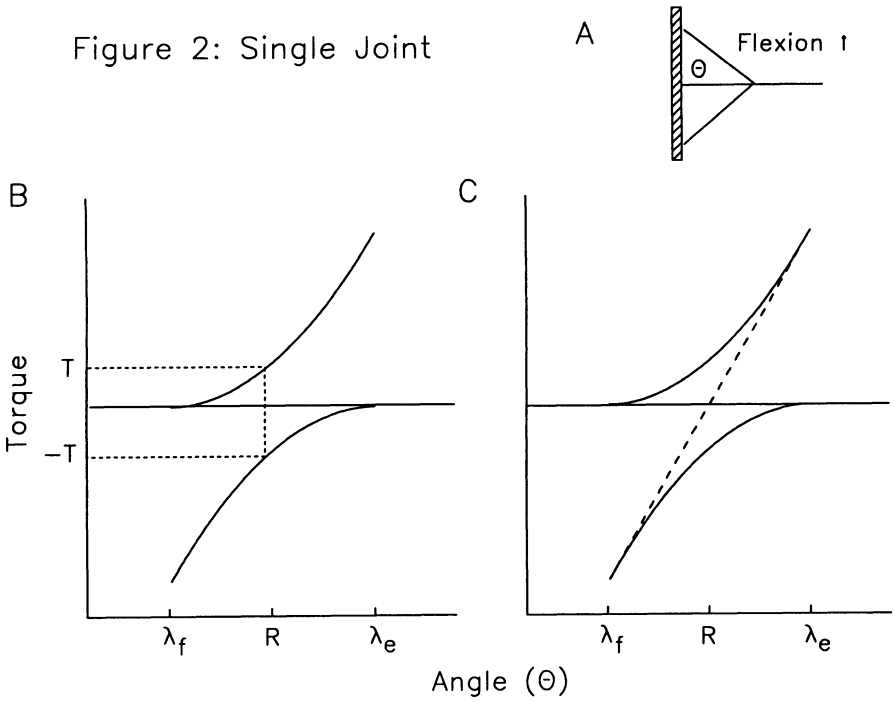

system. If the limb is perturbed into extension (increasing Θ) then the torques produced by the flexor and extensor muscles will increase and decrease respectively and a net flexion torque will restore the system towards equilibrium. Conversely, if the system is perturbed in flexion (decreasing Θ) then the extensor torque will increase while the flexor torque decreases and a net extensor torque will result.

We may make use of Figure 2b to illustrate two orthogonal ways in which the nervous system can centrally control the system. First, by shifting λ_f and λ_e and the corresponding torque-angle curves in opposite directions the nervous system can alter the level muscle of co-activation without changing the equilibrium angle. Second, by shifting λ_f and λ_e in the same direction, the nervous system can change the equilibrium angle without altering the level of muscle co-activation. Thus, in principle - and surely in practice, central signals to the motoneuron pools of both muscles can independently control the equilibrium joint angle as well as the level of muscle co-activation or co-contraction.

Figure 2c illustrates the static relationship between the level of muscle co-activation and joint stiffness. By summing the two muscle torque-angle curves we obtain the total torque-angle relationship for the joint as a whole. It can be shown that when the level of co-activation is

increased the slope of the torque-angle relationship for the joint increases. The slope of this relationship represents joint stiffness. Thus, joint stiffness can be controlled independently of joint angle.

In the two-joint planar arm model we have included three pairs of antagonist or opposing muscles. These include a pair of single-joint antagonists at both the shoulder and elbow and a pair of double-joint antagonists spanning both joints. In addition, the two-joint model includes a full geometric and mechanical description of the planar arm; position and velocity (i.e., damping) sensitive afferent feedback; and muscle properties (e.g., relaxation). Central signals specify the equilibrium posture of the arm in terms of the position of the hand in extrinsic coordinates. The corresponding equilibrium joint angles are determined from limb geometry. Central control signals also specify the levels of co-activation for the three antagonist muscle pairs. For a complete description of the two-joint planar model see Feldman, Adamovich, Ostry & Flanagan (1990) and Flanagan, Ostry & Feldman (1990). For a general account of the mechanisms underlying the λ model see Feldman (1986).

2. Method

Subjects were asked to make rapid arm movements to illuminated targets (LEDs) inlaid in a horizontal surface at a level just below the shoulder. They were instructed not to make any corrective movements. Both single-step targets and double-step targets with inter-stimulus intervals (ISIs) of 50, 75, 100, 125, 175, 250, 350 and 700 ms were presented. Single- and double-step trials were randomly mixed. The position of the single-step targets and the position of the second target in the double-step trials were randomly varied.

The three-dimensional position of infrared emitting diodes (IREDS) attached to the hand, wrist, forearm and upper arm were recorded using the Watsmart system at 400 Hz. In addition, electromyographic (EMG) activity was recorded at 1200 Hz for the biceps, triceps, pectoralis, and posterior deltoid muscles. However, in this paper only the kinematics of the hand will be reported. The experiments took place in a darkened room to limit visual feedback of the position of the limb. The target surface was painted matt black and black infrared absorbing form was used to reduce infrared reflections. Position data were numerically filtered using a Butterworth low-pass filter with a cutoff frequency of 20 Hz. The filtered data were then numerically differentiated with a second-order least squares method.

3. Results and Discussion

3.1. MOVEMENTS TO CO-ALIGNED CENTRAL TARGETS

This section of the results deals with single- and double-step movements involving a proximal and a distal target located centrally with respect to the subject. The start position was also located centrally 5 cm in front of the body. Thus, the two targets and the start position were co-aligned in the mid-sagittal plane. The proximal target was 30 cm from the start position and the distal target was 45 cm from the start position.

The Figure 3a shows position and velocity records for a double-step movement with a 700 ms ISI directed initially to the proximal target and then to the distal target. Two distinct movements can be observed. In Figure 3b, simulated position and velocity records corresponding to the

Figure 3: Double-Step Motion

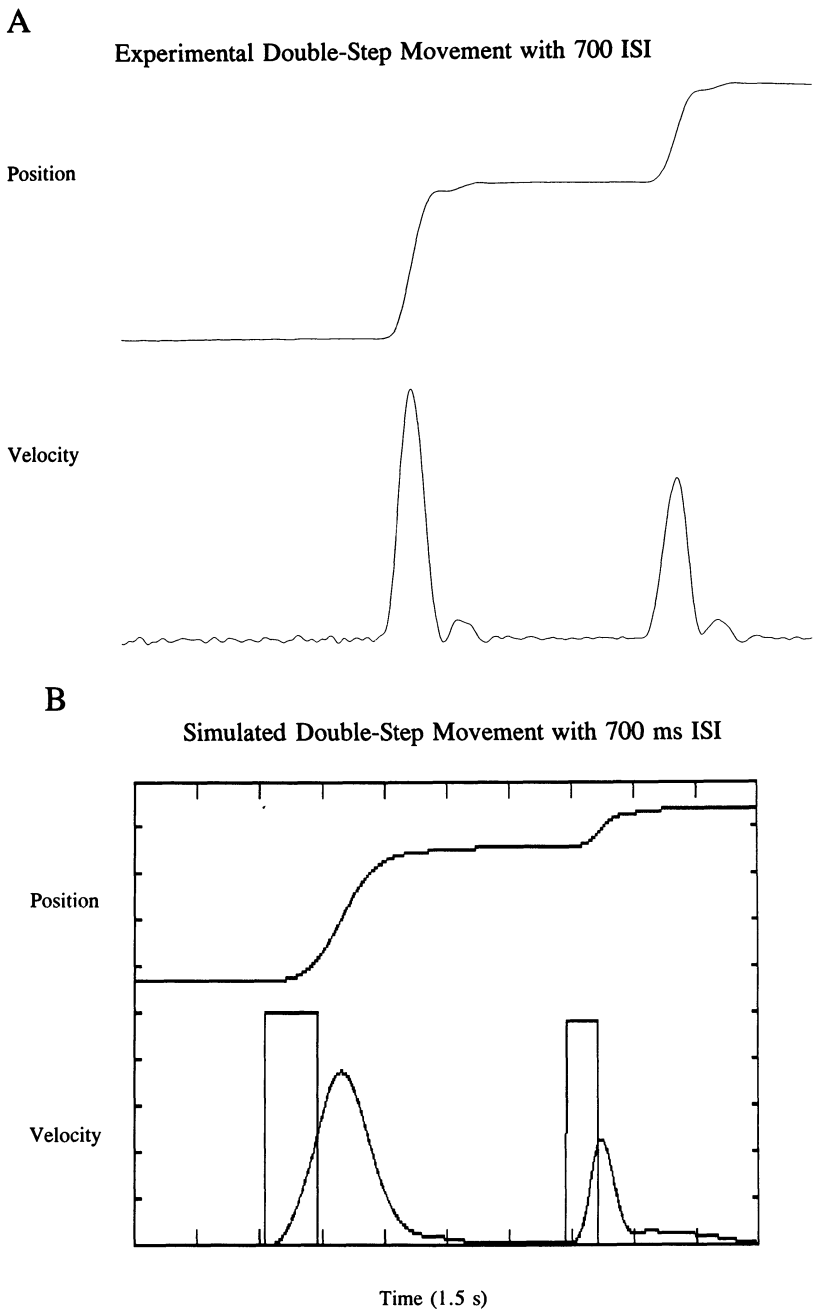

experimental records shown Figure 3a are presented. The model is able to produce smooth bell-shaped velocity profiles consistent with the experimental data.

Figure 4 outlines the predictions of the model for rapid movements of two different amplitudes. Figure 4a shows the equilibrium position of the hand (solid traces) and the predicted actual position of the hand (dotted traces) for a small and a large amplitude movement. The corresponding equilibrium hand velocity profiles are presented in Figure 4b. We assume that the equilibrium position of the hand is shifted at a constant rate in a straight line towards the illuminated target. Moreover, in the case of rapid movements, we assume that the rate of shift is independent of movement amplitude; thus movement amplitude is determined by the duration of the shift. The predicted actual hand positions for the small and large amplitude movements will coincide over the initial phase of the movement (up until the equilibrium position of the hand reaches the proximal target). This prediction was tested experimentally. An advantage of constant velocity shifts in the equilibrium position of the hand is that - in contrast to the minimum jerk model (Flash, 1987) - amplitude need not be specified prior to the initiation of equilibrium shift.

Experimental hand speed profiles (i.e., tangential velocity profiles) for two subjects are presented in Figure 5. The curves have been aligned so that they start at the same time. In all cases, movement onset was taken at the point when the hand speed reached an absolute threshold of .2 m/s. Hand speed profiles for single-step movements to the proximal (thick traces) and distal (light traces) targets are shown in 5a. Consistent with the model prediction, these two sets of profiles are similar over the initial phase of the movement and then diverge. Thus, the rate of shift of the equilibrium position of the hand appears to be unaffected by movement amplitude.

We assume that the equilibrium position of the hand is shifted at a constant rate (in a straight line) towards the presently illuminated target. When the target shifts distally early in the trial, the equilibrium position of the hand simply continues shifting at the same rate towards the second (more distal) target. Therefore the model predicts that double-step movements with small ISIs between the first (proximal) and second (distal) targets should be equivalent to single-step movements to the distal target. This prediction was tested by comparing these double-step movements with single-step movements to both the proximal and the distal targets.

Figure 5b shows hand speed profiles for single-step movements to the proximal target (thick traces) and double-step movements to the proximal and then the distal target with an ISI of 70 ms (thin traces). As expected, these two sets of profiles are similar over the first part of the movement and then diverge. The pattern is similar to that shown in Figure 5a. In Figure 5c, the hand speed profiles for single-step movements to the distal target (thick traces) and the same double-step movements (thin traces) are presented. With a few exceptions, the two sets of profiles are similar as predicted by the model. This suggests that, in the case of the double-step movements, the shift in the equilibrium position of hand is simply continued, at the same rate, towards the second target.

3.2. MOVEMENTS INVOLVING CHANGES IN TARGET DIRECTION

The second part of the results deals with double-step movements in which the position of the second target requires the subject to change movement direction. The same start position and initial target as above were used. Thus, the first target was positioned 30 cm in front of the subject. The second target was positioned either 30 cm to the left or 40 cm to the right of the first target with respect to the subject.

Flash (1990) has modelled double-step movement trajectories as the superposition of two

Figure 4: Model Predictions

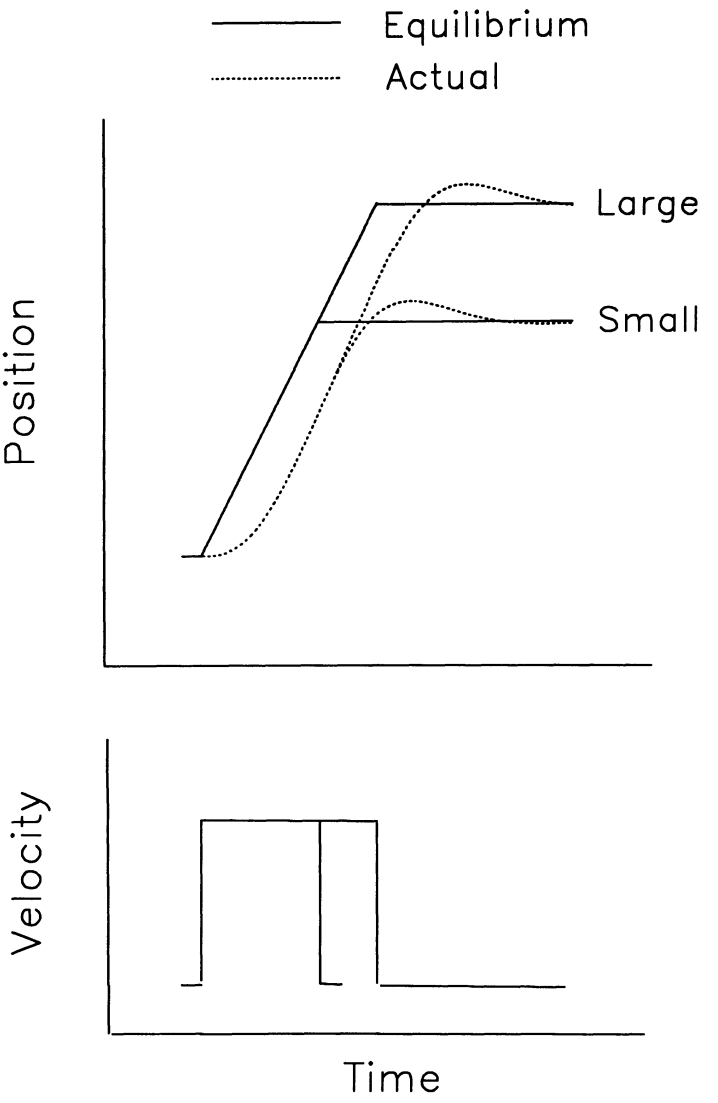

Figure 5: Motions to Co-aligned Targets

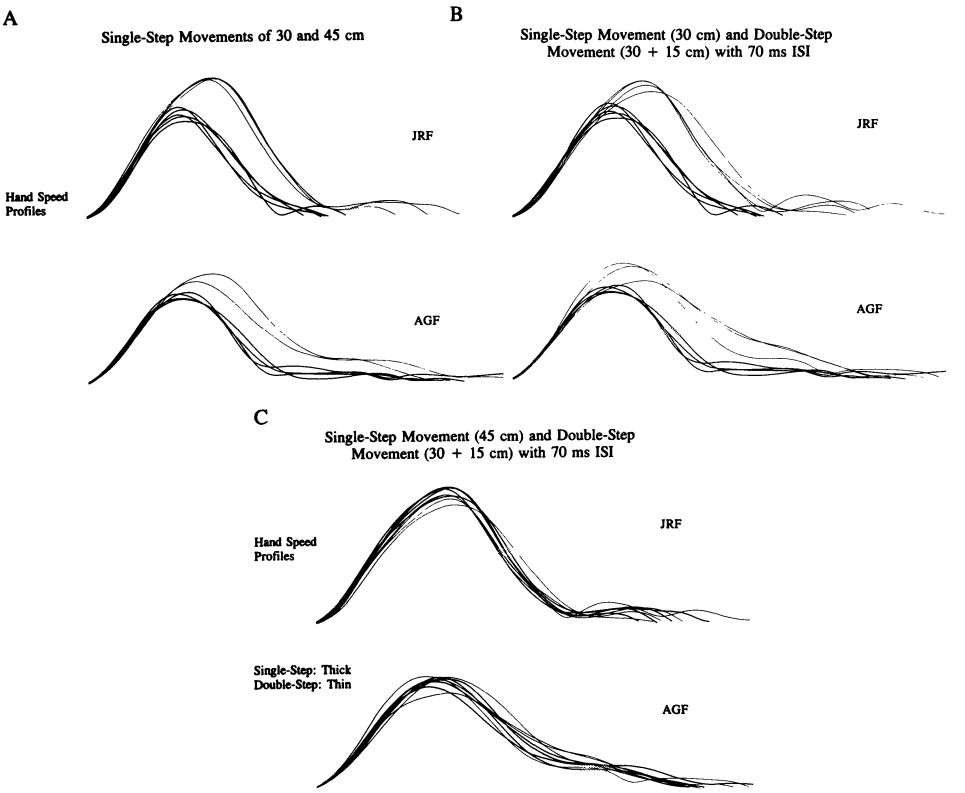

single-step trajectories. The first is from the start position to the initial target and the second is from the initial target to the final target. Both of the superimposed trajectories are assumed to have straight line hand paths and smooth bell-shaped hand speed profiles. The time at which the second trajectory is superimposed on the first will depend on the ISI. This kinematic model can account well for the curved hand paths and smooth bi-modal hand speed profiles observed in double-step movements with sufficiently large ISIs. However, we suggest that curved hand paths and smooth hand speed profiles result from movement dynamics as the equilibrium position of the hand is shifted at a constant rate in the direction of the first target and then (at the same rate) in the direction of the second target. Thus, the equilibrium shift to the first target is terminated as the shift to the second target is initiated.

Figure 6a shows experimental hand paths in the horizontal plane for double-step movements involving both final targets with a range of ISIs. With larger ISIs the hand achieves the first

Figure 6: Motions with Changing Target Direction

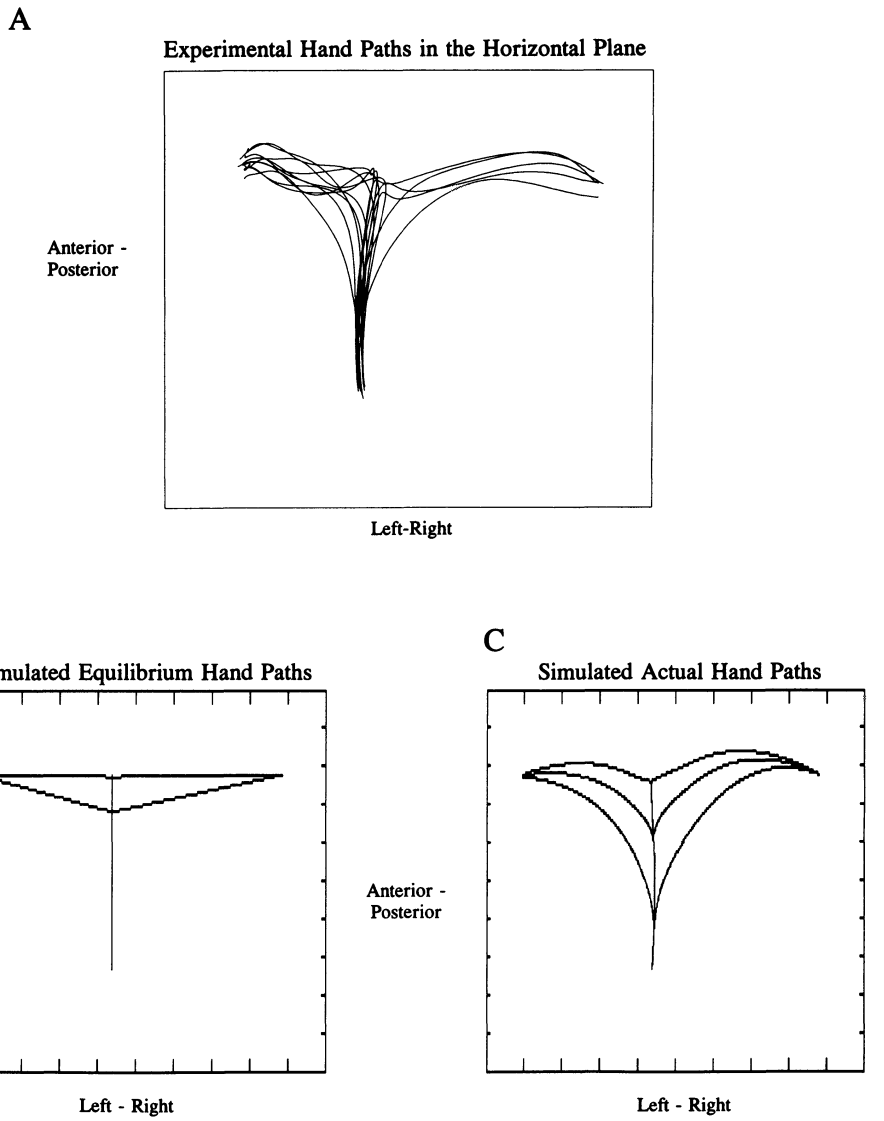

target before moving to the second target whereas with small ISIs the hand begins to curve towards the second target before reaching the first target. Simulated equilibrium and actual hand paths corresponding to these experimental paths are shown in Figure 6b and Figure 6c respectively for different ISIs. With the shortest ISIs, the equilibrium position of the hand shifts in the direction of the second target before it reaches the first target. With intermediate ISIs, the equilibrium position of the hand achieves the first target but is shifted towards the second target before the actual hand position reaches the first target. Finally, with large ISIs, both the equilibrium hand position and the actual hand position reach the first target. Figure 6c illustrates that constant rate shifts in the equilibrium position of the hand directed in a straight line towards the presently illuminated target can account - qualitatively - for the smoothly curved hand paths that are observed experimentally.

4. Conclusions

We suggest that the two-joint horizontal arm movements are planned in coordinates corresponding to the equilibrium position of the hand. In the case of rapid goal-directed movements, it is argued that the equilibrium position of the hand is shifted at a constant rate in a straight line directed towards the presently illuminated target. We have demonstrated that these constant rate shifts in the equilibrium position of the hand can produce predicted actual hand speed profiles that are smooth and bell-shaped. Thus, we do not believe that smoothness is explicitly planned by the central nervous system. Rather, smooth motions arise as a consequence of the dynamic interaction of central commands, afferent reflex mechanisms, muscle properties and limb mechanics. Finally, it is proposed that for rapid goal-directed arm movements, the rate of shift in the equilibrium position of the hand is independent of movement amplitude.

5. References

Feldman, A.G. (1986). Once more on the equilibrium-point hypothesis (λ model) for motor control. *Journal of Motor Behavior*, 18, 17-54.

Feldman, A.G., Adamovich, S.V., Ostry, D.J., & Flanagan, J.R. (1990). The origin of electromyograms - explanations based on the equilibrium point hypothesis. In J. Winters & S. Woo (Eds.), *Multiple muscle systems: biomechanics of movement organization*. Springer-Verlag.

Flanagan, J.R., Feldman, A.G., & Ostry, D.J. (1990). Control of human jaw and multi-joint arm movements. In G. Hammond G (Ed.), *Cerebral control of speech and limb movements*. Springer-Verlag.

Flash, T. (1987). The control of hand equilibrium trajectories in multi-joint arm movements. *Biological Cybernetics*, 57, 57-74.

Flash, T. (1990). The organization of human arm trajectory control. In J. Winters & S. Woo (Eds.), *Multiple muscle systems: biomechanics of movement organization*. Springer-Verlag.